Ab Initio Calculations and Force Field Development for Computer Simulation of Polysilanes

H. Sun

Biosym Technologies, Inc., 9685 Scranton Road, San Diego, California 92121

Received August 1, 1994; Revised Manuscript Received October 24, 1994®

ABSTRACT: An all-atom force field for computer simulation of polysilanes, including their alkyl and phenyl side-chain derivatives, is developed based on *ab initio* calculations and liquid-state simulations of simple silane molecules. Validation of the force field shows good agreement with experimental data of isolated and condensed silanes and polysilanes. Conformational structures and energies of polysilane and poly(dimethylsilane) were studied based on *ab initio* calculations and the force field developed. It is found that the *all-trans* backbone of isolated polysilane is more stable than the *gauche*. Poly(dimethylsilane) has a helical backbone in the gas phase but is *all-trans* in the crystal due to the interchain nonbonded interaction.

I. Introduction

Polysilanes have been the focus of increasing attention recently due to their unusual electrical and optical properties and potential applications. In particular, solid-state molecular conformations and electronic absorption of dialkyl-substituted polysilanes have been studied extensively.[1−6] It is reported that these polymers adopt different backbone conformations with respect to the lengths of their side chains. With fewer than four carbons in their side chains, poly(dimethylsilanes) (PDMS), poly(diethylsilanes) (PDES), and poly(di-*n*-propylsilane) (PDnPS) are *all-trans* and absorb at about 330−340 nm.[1,2] Polysilanes with four and five carbons in their side chains adopt 7/3 helical conformations, with the absorption peaks at about 320 nm.[3,4] With six to eight carbons in their side chains, polysilanes adopt *all-trans* again and absorb at about 373 nm.[5,6] It has been suggested[1] that the mechanism of forming an *all-trans* conformation is different in the two cases. For the higher homologous polymers, interactions between the side chains determine the molecular conformation, while for the lower homologous polymers, σ-delocalization of the electrons along the backbone is the driving force. The thermochromism of polysilanes in solution has also been studied by several research groups.[4,7−11] It has been found that symmetrically alkyl-substituted polysilanes absorb at about 355 nm at low temperatures and abruptly shift to about 315 nm above the transition temperatures; asymmetrically alkyl-substituted polysilanes absorb around 320−340 nm under their transition temperatures and slightly shift to about 310 nm as the temperatures increase; the transition temperatures are rather broad in the later cases. The mechanisms of the thermochromism and the order−disorder transition of polysilanes in solutions have been a subject of extensive discussions.[11] Schweizer et al. applied a microscopic statistical mechanics theory and proposed that the driving force of the order−disorder transition is primarily due to the conformationally dependent polymer−solvent interactions.[11]

Many theoretical calculations have been performed to study chain conformations of polysilanes. However, most calculations reported in the literature so far are based on empirical, semiempirical, and low-level *ab initio* methods. Consequently, controversial results have been reported. Using an empirical force field, Damewood and West[12] found the *all-gauche* conformation to be the lowest energy conformation for both polysilane and its dimethyl derivative. Cui, Karpfen, and Kertesz[13] carried out semiempirical AM1 calculations and found that *all-trans* conformations are lower in energy than the *gauche* conformations for both polysilane and poly(dimethylsilane). With MNDO and *ab initio* HF/3-21G and HF/3-21G* calculations, Welsh and Johnson[14] predicted that the most stable chain conformations are *all-trans* for polysilanes. However, their MNDO results indicate the most favorable chain conformation of poly(dimethylsilane) is a helix (with a skew angle of 170°). More rigorous *ab initio* studies of silanes have been reported by Mintmire and Ortiz.[15] These authors showed that the optimized conformations depend on the method of calculations. The *trans* conformation is more stable at HF/3-21G and HF/6-31G* levels of theory, but the *gauche* conformation is slightly more stable at the MP2/6-31G* level. All of these calculations are performed on isolated oligomers only. Recently, Patnaik and Farmer[16] conducted empirical force field calculations for isolated and crystalline PDMS. They found that the isolated PDMS adopts a 15/7 helical conformation, but the most stable crystalline PDMS has an *all-trans* chain conformation, indicating that the driving force leading to the *all-trans* conformation of PDMS is the intermolecular interaction.

Generally speaking, to accurately calculate the conformational properties is a difficult task. It is known that semiempirical methods—MNDO, AM1, PM3, etc.[17−19]—do not consistently yield agreement with each other nor with the experimental data. *Ab initio* techniques[20] are more reliable and systematically improvable. However, only high-level calculations with large basis sets and corrections for electron correlation yield reliable results.[21] Consequently, the calculations quickly reach hardware limitations as the size of the molecule increases, so that only small, isolated molecules can be calculated accurately with today's computers.

To understand and to predict properties of macromolecules, computer simulation techniques—molecular mechanics, molecular dynamics, Monte Carlo, etc.—are being used by many research groups. Because the number of atoms to which these methods can be applied is several orders of magnitude larger than that of the

® Abstract published in *Advance ACS Abstracts,* January 1, 1995.

0024-9297/95/2228-0701$09.00/0

ab initio techniques, these simulation techniques have been and will continue to be very important in computational chemistry. An underlying issue of all atomistic simulations is the quality of the force field, which consists of a set of analytical function forms and parameters and provides a detailed description of inter- and intramolecular interactions as functions of molecular structures and relative positions.

Although empirical force fields can be parametrized accurately,[22-26] the quality of the force field depends highly on the availability of the experimental data which are used to parametrize. In the absence of experimental data, one usually finds that the calculations involve some "estimated" or "transferred" parameters, which may lead to inaccurate results. To this end, a valuable approach which overcomes the difficulties mentioned above is to derive a good force field based on high-quality *ab initio* calculations.[27-30] In our view, a force field derived in such a way plays a uniquely important role—it builds a bridge between the high-quality *ab initio* calculations and the large-scale property predictions.

There has been a growing interest in force field development in recent years.[22-49] This paper reports a CFF93 type,[27] all-atom force field for computer simulations of polysilanes and their alkyl- and phenyl-substituted derivatives. The present force field uses much more complex functional forms than those of the earlier developed force fields, such as MM2,[22] CVFF,[24] etc.: anharmonic terms are used for bonds and angles, Fourier expansion is employed for torsions, extensive cross-coupling terms are included, and the nonbonded interactions are explicitly written in terms of both van der Waals forces and electrostatic interactions. Consequently, the present force field is much more flexible and potentially able to predict not only equilibrium geometries and conformational energies but also electrostatic potentials and vibrational frequencies. In addition, since the quantum mechanical *ab initio* calculations can provide large amounts of information with reasonable accuracy, the parametrization of a very complex force field becomes much easier than with the traditional approach.

In order to develop the force field, extensive *ab initio* calculations were carried out for silanes and alkyl- and phenyl-substituted silanes. In comparison with the *ab initio* calculations of silanes reported in the literature,[12,15] the present calculations were performed at higher levels of accuracy. Hopefully, the results provide a more reliable theoretical discussion of conformational structures and energies of polysilanes. Another main object of this paper is to present the force field. Except for some simple empirical force fields,[12,16] this is the first systematically parametrized, fully relaxed force field for polysilanes. Finally, this paper reports some preliminary molecular mechanics and molecular dynamics applications using this new force field.

All calculations reported in this paper were conducted on an IBM RISC/6000 550 workstation. The *ab initio* software packages TURBOMOLE[50] and GAUSSIAN90[51] with the direct SCF method were used. The nonlinear least-squares fits of the valence and cross-coupling parameters were conducted by using Biosym's software package PROBE.[52] All molecular mechanics and molecular dynamics calculations were conducted by using DISCOVER.[52]

II. Quantum Mechanics Calculations

Geometry optimizations were conducted by using the gradient minimization algorithm provided with the *ab initio* software packages. Unless explicitly stated, all optimizations reported in this paper were conducted in full—all degrees of freedom were relaxed, and no constraints except symmetries were imposed during these calculations. The total energies, analytic gradients, and Hessian matrices were calculated. In order to be consistent with our research program and to transfer already derived parameters[27-30] directly, Hartree–Fock calculations with the 6-31G* basis functions[53] (HF/6-31G*) were primarily used for the parametrizations. However, in order to probe the conformational properties for which high-quality *ab initio* calculations must be employed to obtain reliable information, triple-ζ basis sets[54] and the Møller–Plesset perturbation theory (MP2, MP3, and MP4)[55] were used for some of these calculations. The triple-ζ basis set was augmented with polarization functions. A smaller set, called TZ2P, is augmented with two polarization functions (Si, 2.0, 0.5; C, 0.44, 1.58; H, 0.44, 1.58).[56] Another, TZ2PF, is further augmented with f polarization functions for heavy atoms (Si, 1.0; C, 0.96).

Table 1. Comparison of *ab Initio* and Experimental Geometric and Energetic Parameters of Disilane

method	Si–Si	Si–H	H–Si–H	$E_{barrier}$
HF/6-31G*	2.352	1.478	108.5	0.95
HF/TZ2P	2.355	1.477	108.6	0.97
MP2/6-31G*	2.335	1.487	108.5	1.08
MP2/TZ2P	2.330	1.472	108.7	1.19
MP4/TZ2P	2.337	1.477	108.6	1.18
MP3 energy				1.18
MP2 energy				1.18
MP2/TZ2PF	2.320	1.470	108.6	1.21
MP4/TZ2PF	2.327	1.475	108.6	1.20
MP3 energy				1.19
MP2 energy				1.20
expt	2.327	1.482	107.85	1.26

The influences of using different basis sets and including electron correlations need to be understood before these methods are used to study the molecular structures and conformational energies. A calibration of these methods was carried out by performing calculations on disilane. Disilane is a good test model because of its small size and the available gas-phase experimental data.[57,58] The minimum-energy structure of disilane has D_{3d} symmetry, the transition state for rotation about the Si–Si bond has D_{3h} symmetry, with the hydrogens in the eclipsed position. The rotation barrier is 1.26 kcal/mol, based on the measurements of gas-phase Raman spectroscopy.[57] Both minimum-energy and transition states were optimized. The structural parameters and energy barriers obtained are listed in Table 1.

Comparison of the calculated results with the experimental values shows that significant deviations, in both structural and energetic values, are found at the HF/6-31G* level of theory. The Si–Si bond length is too long and the barrier of rotation is too low at this level. Simply expanding the basis set from 6-31G* to TZ2P, with the HF method, does not improve the quality of calculation. In contrast, inclusion of the electron correlation significantly reduces the deviations. As shown in Table 1, most MP calculations yield fairly good agreement with the experimental data. The moderately large deviations found for the Si–H bond and the H–Si–H angle are not surprising, because of the difficulty in measuring the positions of the hydrogen atoms and the finite temperature effect. The best agreements were achieved at the MP4/TZ2PF level. The bond length of Si–Si agrees extremely well with the experimental data, and the energy barrier is only 0.06

kcal/mol lower than the experimental value. It is of interest to point out, however, that at a lower level, MP2/TZ2P, the calculated results are in very good agreement with the much higher (and more expensive) MP4/TZ2PF results. Between the MP2/TZ2P and MP4/TZ2PF levels, using either a larger basis set with MP2 or a smaller basis set with MP4 does not give good results; the bond lengths of Si–Si are either too long or too short, although the energy differences are minimal.

III. Force Field Method and Parametrization

Methodology. Since the methodology used to develop a CFF93-type force field has already been reported in the literature,[27–30] only a very brief description is given here. A two-step procedure is used to parametrize the force field. First, a quantum mechanical force field (QMFF) was developed by least-squares fitting to the *ab initio* data calculated for a set of selected model compounds that sample the potential energy surfaces. The *ab initio* data include electrostatic potentials, energies, and first and second derivatives of the energies. Then, the quantum mechanical force field was scaled by a set of generic parameters to correct the systematic errors of the *ab initio* calculations.

The functional forms of this force field are given as:

$$E_{\text{total}} = \sum E^{\text{b}} + \sum E^{\text{a}} + \sum E^{\text{t}} + \sum E^{\text{o}} + \sum E^{\text{bb}'} + \sum E^{\text{ba}} + \sum E^{\text{bt}} + \sum E^{\text{aa}'} + \sum E^{\text{at}} + \sum E^{\text{aa't}} + \sum E^{\text{vdw}} + \sum E^{\text{elec}}$$

where

$$E^{\text{b}} = \sum_{n=2}^{4} k_n^{\text{b}}(b - b_0)^n$$

$$E^{\text{a}} = \sum_{n=2}^{4} k_n^{\text{a}}(\theta - \theta_0)^n$$

$$E^{\text{t}} = \sum_{n=1}^{3} k_n^{\text{t}}(1 - \cos n\phi)$$

$$E^{\text{o}} = k^{(\text{o})}(\chi - \chi_0)^2$$

$$E^{\text{bb}'} = k^{\text{bb}'}(b - b_0)(b' - b'_0)$$

$$E^{\text{ba}} = k^{\text{ba}}(b - b_0)(\theta - \theta_0)$$

$$E^{\text{aa}'} = k^{\text{aa}'}(\theta - \theta_0)(\theta' - \theta'_0)$$

$$E^{\text{bt}} = (b - b_0)\sum_{n=1}^{3} k_n^{\text{bt}} \cos n\phi$$

$$E^{\text{at}} = (\theta - \theta_0)\sum_{n=1}^{3} k_n^{\text{at}} \cos n\phi$$

$$E^{\text{aat}} = k^{\text{aat}}(\theta - \theta_0)(\theta' - \theta'_0)\cos\phi$$

and

$$E^{\text{vdw}} = \epsilon[2(r^*/r)^9 - 3(r^*/r)^6]$$

$$E^{\text{elec}} = Q_i Q_j / r_{ij}$$

Table 2. Model Compounds Selected for Sampling Potential Surfaces of Polysilanes

molecule abbrev	name	chemical formula
S	silane	SiH_4
DS	disilane	SiH_3SiH_3
TrS	trisilane	$SiH_3SiH_2SiH_3$
TeS	tetrasilane	$SiH_3SiH_2SiH_2SiH_3$
MS	methylsilane	SiH_3CH_3
ES	ethylsilane	$SiH_3CH_2CH_3$
DMS	dimethylsilane	$SiH_2(CH_3)_2$
MDS	methyldisilane	$SiH_3SiH_2CH_3$
EDS	ethyldisilane	$SiH_3SiH_2CH_2CH_3$
DMTrS	2,2-dimethyltrisilane	$SiH_3Si(CH_3)_2SiH_3$
PS	phenylsilane	$C_6H_5SiH_3$
PDS	phenyldisilane	$C_6H_5SiH_2SiH_3$
MPTrS	2-methyl-2-phenyltrisilane	$SiH_3Si(CH_3)(C_6H_5)SiH_3$
DPTrS	2,2-diphenyltrisilane	$SiH_3Si(C_6H_5)_2SiH_3$

The total energy is divided into three major categories: (a) contributions from each of the internal valence coordinates, (b) cross-coupling terms between internal coordinates, and (c) nonbonded interactions. The valence energies consist of terms from distortions of bond lengths E^{b}, bond angles E^{a}, out-of-plane bending angles E^{o}, and torsion angles E^{t}. Both bond and angle terms contain up to quartic terms to characterize anharmonic features. The torsion function is represented by a symmetric Fourier expansion. The out-of-plane function is a simple harmonic function. Several cross-coupling terms are used in this force field: E^{bb}, E^{ba}, $E^{\text{aa}'}$, E^{bt}, E^{at}, and $E^{\text{aa't}}$ represent bond–bond, bond–angle, angle–angle, bond–torsion, angle–torsion, and angle–angle–torsion coupling terms,[27] respectively. The nonbonded energies include intramolecular nonbonded interactions, which are interactions between any pair of atoms that belong to the same molecule but are separated by at least two intervening atoms, and intermolecular nonbonded interactions, which are the interactions between any pair of atoms that belong to different molecules. The nonbonded energies are subsequently divided into van der Waals interactions E^{vdw} and electrostatic interactions E^{elec}. A 9–6 Lennard-Jones function[59] is used to represent the van der Waals forces, while the electrostatic interaction is written in the form of a standard Coulombic interaction with partial atomic charges. In order to obtain transferable parameters, charges are further written as a sum of bond increments δ_{ij}, which are defined as a charge displacement from atom i to atom j. For each atom i, the charge is a sum of δ_{ij},

$$Q_i = \sum_j \delta_{ij}$$

where j runs over all atoms that are directly bonded to atom i. Because of the definition, the bond increment for any pair of like atoms is zero.

Parametrization of the Quantum Mechanics Force Field (QMFF). Fourteen model compounds of silanes and alkyl- and phenyl-substituted silanes were calculated. The names, the abbreviations used in this paper, and the chemical formulas of these model compounds are given in Table 2. Some important bond lengths and angles of the optimized structures are summarized in Table 3. Examination of the data in Table 3 shows that most internal coordinates are quite insensitive to the substituents. The exception is the bending angle Si–Si–Si, which changes significantly from about 106° to 113°, showing large flexibility of this bending angle.

The atomic partial charges were derived by fitting to the *ab initio* electrostatic potentials.[60–69] Table 4 lists

Table 3. Mean Values of the HF/6-31G* Optimized Structural Parameters of Silane Model Compounds

molecule	bond length			bond angle			
	Si–H	Si–Si	Si–C	Si–Si–Si	H–Si–H	C–Si–C	C–Si–H
				Silanes			
S	1.475			109.5			
DS	1.478	2.352			108.5		
TrS	1.478	2.357		112.7	108.5		
	1.481[a]				107.6[a]		
TeS	1.478	2.357		112.8	108.5		
	1.482	2.361			107.4		
				Alkyl Derivatives			
MS	1.478		1.889		108.3		110.6
ES	1.479		1.893		108.4		110.7
DMS	1.481		1.890		107.6	111.4	109.4
MDS	1.480	2.355	1.896		108.2		
	1.481[a]				108.9[a]		109.7[a]
EDS	1.480	2.356	1.900		108.1		
	1.482[a]				109.0[a]		109.7[a]
DMTrS	1.481	2.363	1.904	109.7	107.9	109.5	
				Phenyl Derivatives			
PS	1.477		1.882		108.5		110.4
PDS	1.479	2.355	1.890		108.2		
	1.481[a]				106.5[a]		109.6[a]
MPTrS	1.480	2.363	1.900	109.8	108.1	110.4	
			1.903[b]				
DPTrS	1.479	2.366	1.902	106.2	108.0	111.5	

[a] SiH_2 group only. [b] With methyl carbon.

Table 4. ESP Charges Calculated for the Model Compounds

molecule	Si		H(–Si)		C		H(–C)	
DS	$Si(-SiH_3)$	0.383	H	−0.1275				
TrS	$Si(-SiH_3)$	0.483	$H(-SiH_3)$	−0.147				
	$Si(-SiH_2-)$	0.109	$H(-SiH_2-)$	−0.095				
MS	$Si(-SiH_3)$	0.734	$H(-SiH_3)$	−0.196	$C(-CH_3)$	−0.425	$H(-CH_3)$	0.093
MDS	$Si(-SiH_3)$	0.331	$H(-SiH_3)$	−0.122	$C(-CH_3)$	−0.311	$H(-CH_3)$	0.070
	$Si(-SiH_2-)$	0.454	$H(-SiH_2-)$	−0.159				
DMS	$Si(-SiH_2-)$	0.886	$H(-SiH_2-)$	−0.233	$C(-CH_3)$	−0.594	$H(-CH_3)$	0.126
PS	$Si(-SiH_3)$	0.623	$H(SiH_3)$	−0.165	C(–SiC–)	−0.134	H(–CH–)	0.135
					C(–CH–)	−0.135		
DMTS	$Si(SiH_3)$	0.393	$H(SiH_3)$	0.141	$C(CH_3)$	−0.511	$H(CH_3)$	0.119

the mean values of the charges calculated for the optimized structures of selected model molecules. The fitting was conducted by using TURBOMOLE,[50] with HF/6-31G* wavefunctions. A spherical grid model, in which the grid points were placed symmetrically on several concentric spherical shells around each of the nuclei, was used in this study. The first shell was placed at a distance 1 Å greater than the standard van der Waals radii from each of the nuclei in the molecule. Ten more shells of grids were placed at distances of 2, 3, 4, 5, 6, 7, 8, 10, 12, and 16 Å greater than the van der Waals radii. A total of 4000 points was placed on each of the shells. However, in the region where two or more spheres overlap, some grid points were removed from the region to avoid oversampling. The least-squares fits were generally satisfactory, with the root-mean-square (rms) deviations below 0.25 kcal/mol.

The values given in Table 4 were averaged and scaled by a generic scaling factor of 0.9 which was obtained by a comparison of the dipole moments between HF/6-31G* values and experimental data for a large group of organic compounds including ethers, esters, acids, alcohol, aldehydes, and ketones.[70] The resulting parameters—bond increments—are given in Table 5.

Another part of the nonbonded interaction is the van der Waals term. It is difficult to obtain the van der Waals parameters directly from the *ab initio* calculations because with the Hartree–Fock approximation one cannot treat the dispersion force correctly,[20] and high-level calculations are not feasible because of the amount of computation. In the CFF93 force field, the van der Waals parameters are generally determined by fitting to low-temperature crystal structures and sublimation energies.[27,28] Due to the lack of such experimental data for silanes, liquid structures and energies at normal temperatures were used to determine the van der Waals parameters in this study. This was accomplished by using the following procedure: First, an initial guess for these parameters was made based on a literature survey;[16,22] then these parameters, together with charge parameters, were fixed, while the valence parameters were derived; finally, the van der Waals parameters were refined by comparing the simulated results of liquid-state silanes with experimental data. The initial and refined nonbonded parameters are given in Table 5.

Table 5. Nonbonded and van der Waals Parameters

Nonbonded Parameters

	bond increment (electron)
Si–H	0.126
Si–C	0.135
Si–Cp	0.117
C–H	−0.053
Cp–H	−0.140

van der Waals Parameters

	initial guess		refined	
	ϵ (kcal/mol)	D (Å)	ϵ (kcal/mol)	D (Å)
Si	0.160	4.50	0.190	4.450
H	0.020	2.995	0.023	2.940

Table 6. Comparison of Total Energies (kcal/mol) between *ab initio* HF/6-31G* (HF) and Quantum Mechanics Force Field (FF) Calculations

	DS		TrS		MS		MDS		DMS		DMTrS		PS	
conf	HF	FF	HF	FF	HF	FF	HF	FF	HF	FF	HF	FF	HF	FF
0	0.0	0.0	0.0	0.0	0.0	0.0	0.0	0.0	0.0	0.0	0.0	0.0	0.0	0.0
1	9.9	10.4	12.5	12.5	15.8	15.7	25.1	25.1	25.8	25.7	36.4	36.6	9.0	8.8
2	14.7	14.6	21.7	22.2	27.5	27.3	16.7	16.9	28.4	28.0	43.3	42.7	5.5	5.4
3	10.0	9.8	21.7	22.1	8.1	8.4	19.8	19.8	16.0	16.2	31.9	32.0	8.9	8.7
4	10.5	10.2	15.7	15.9	16.8	16.4	15.4	15.3	33.5	34.1	31.1	31.6	6.3	6.5
5	15.3	15.1	18.8	18.5	12.1	12.1	17.0	16.7	18.3	17.8	35.2	34.5	9.5	9.5
6	13.8	13.7	20.7	20.6	17.9	18.1	22.9	23.1	37.3	37.1	44.1	44.8	7.9	7.9
7	12.4	12.1	19.5	19.7	10.2	10.0	16.4	16.7	19.6	19.4	33.3	33.1	3.0	3.1
8	11.5	10.9	15.6	15.5	16.5	16.4	23.6	23.4	31.3	31.3	37.7	37.5	6.4	6.6
9	13.1	12.2	12.9	12.6	16.3	16.5	14.1	14.2	22.9	23.3	41.6	42.2	6.2	6.5
10	15.7	16.1	13.9	13.7	19.4	19.2	19.4	19.2	24.7	24.5	30.6	30.4	7.6	7.3
av δE	0.4		0.2		0.2		0.2		0.3		0.4		0.2	
rms δE	0.4		0.3		0.2		0.2		0.3		0.5		0.2	
max δE	1.0		0.5		0.4		0.3		0.6		0.7		0.3	

Table 7. Percentage Errors of the First and Second Derivatives of Energies

	percentage error (%)	
molecule	1st	2nd
DS	7.2940	3.0672
TS	8.2525	3.1501
MS	5.2762	3.4144
MDS	5.3397	2.9716
DMS	5.9915	3.1485
DMTS	7.3901	3.2204
PS	7.4075	3.2676

The valence parameters, including intrinsic and cross-coupling terms, were derived by least-squares fitting to the *ab initio* data. Following the procedure used in developing the CFF93 force field,[27,28] the *ab initio* data base includes not only the optimized structures but also distorted structures which are made by randomly altering the bond lengths, bond angles, and dihedral angles of the fully optimized structures. The maximum displacements of the distortion are 0.1 Å for bond lengths and 15° for bond angles and torsional angles. Seven model molecules, as listed in Table 6, were chosen to sample the energy surfaces. For each of these molecules, 11 conformations, which include 1 optimized structure and 10 distorted structures, were calculated. A total of 53 827 observables were obtained from the calculations for the 77 conformations. The total number of parameters is 320. However, only 115 parameters were adjustable during the fit, while the rest were fixed—some of them were transferred from the alkane and benzene force field and some of them were fixed due to redundancies of the function definitions.

In Table 6, comparisons of the relative total energies are given for each of the conformations of the model compounds. The force field derived at this level is called the quantum mechanics force field (QMFF). It is shown in Table 6 that the QMFF values agree well with the *ab initio* HF/6-31G* results. The average deviation, the root-mean-square deviation (RMS), and the maximum deviation between these two sets of values are also summarized at the bottom of the table.

Table 7 shows the fit quality of the derivatives. The relative deviations (percentage errors) of the first and second derivatives of the total energies between HF/6-31G* and QMFF are given. The errors are less than 7.4% for the first derivatives and 3.4% for the second derivatives. Slightly large deviations of the first derivatives are due to the minimized energy structures which have very small first derivatives.

Using the obtained QMFF, molecular structures and the normal-mode vibrational frequencies were calculated for the model compounds. In Table 8, a summary of the comparisons of structural parameters and vibrational frequencies between the QMFF and the HF/6-31G* results is given. The QMFF optimized structural parameters agree well with the *ab initio* results—the rms values are less than 0.004 Å for bond lengths; less than 1.0° for bond angles, and less than 0.8° for torsional dihedrals. Four deviations—the average deviation, av $d\nu$, the average absolute deviation, av $|\delta\nu|$, the rms deviation, rms $\delta\nu$, and the maximum deviation, max $\delta\nu$—are given for comparison of the vibrational frequencies. The QMFF calculated results are in good agreement with the *ab initio* results.

Modification of the QMFF. Since the calculated results at the HF/6-31G* level of theory contain systematic errors due to the truncation of the basis set and the neglect of the electron correlation,[20] the QMFF parameters are scaled by a set of generic scaling factors[27] which have been obtained by fitting the HF/6-31G* force field to experimental data, as discussed above.

Another important change to the QMFF is the van der Waals parameters which were initially estimated based on a literature survey and fixed during the development of QMFF. The modified nonbonded parameters are given in Table 5, together with the initial guess for comparison. The van der Waals parameters are modified based on the liquid-state simulations for a group of low molecular weight silanes. Two properties are primarily calculated for this purpose: cohesive energies and densities. The simulations were conducted in periodic cubic boxes with the use of the minimum image convention. The sizes of the unit cells are in the range of 20–25 Å, with 600–800 atoms. The cohesive energies were calculated based on canonical ensemble (*NTV*) simulations with the densities fixed at the experimental values;[58] the densities were estimated based on constant pressure (*NPT*) simulations. In both cases, the tail corrections to the truncation of nonbonded interactions in the minimum image simulation were included. The average simulation time was generally more than 200 ps after an equilibrium run of about 100 ps for each of the systems. All calculations were conducted at 300 K.

In Table 9, the calculated cohesive energies are compared with the vaporization energies for the liquids simulated. Since the vaporization energies are measured at the boiling temperatures[58] (also given in this table), we see systematically discrepancy between the calculated and the experimental values. However, the agreement is very good for Si_3H_8 which has a boiling temperature close to 300 K. Also, we see that the

Table 8. Deviations of Structural Parameters and Normal-Mode Frequencies

	DS	TS	MS	MDS	DMS	DMTS	PS
			Structural Parameters				
bond rms (Å)	0.003	0.003	0.001	0.002	0.001	0.004	0.002
angle rms (deg)	0.1	1.0	0.2	0.4	0.3	0.7	0.7
torsion rms (deg)	0.0	0.7	0.0	0.2	0.2	0.8	0.0
			Normal-Mode Frequencies (in 1/cm)				
av $\delta-3.9$	−3.9	0.3	5.1	4.2	13.1	4.0	10.1
av $\lvert\delta\nu\rvert$	26.2	21.8	19.9	17.6	21.4	16.5	21.2
rms $\delta\nu$	30.0	25.7	23.7	21.6	28.9	21.6	25.8
max $\delta\nu$	58.7	56.1	52.3	51.1	69.4	53.5	63.0

Table 9. Comparison of the Cohesive Energies with Experimental Vaporization Energies (Units Are kcal/mol for Energies and g/cm³ for Densities)

	expt[58]			
molecule	density	T_b	δE_{vap}	PCFF: δE (300 K)
Si_3H_8	0.739	326	6.14	6.13
Si_4H_{10}	0.795	381	7.45	7.98
i-Si_4H_{10}	0.792	375	6.74	7.98
Si_5H_{12}	0.827	426	9.12	9.85
Si_6H_{14}	0.847	467	10.45	12.04

Table 10. Calculated Densities (in g/cm³)

molecule	expt[58]	PCFF	pressure (bar)
Si_3H_8	0.739	0.739	550
Si_4H_{10}	0.795	0.784	630
i-Si_4H_{10}	0.792	0.796	630
Si_5H_{12}	0.827	0.817	675
Si_6H_{14}	0.847	0.850	700

differences monotonically increase as the boiling temperature increases from the Si_4H_{10} to Si_6H_{14}. The calculated densities are given in Table 10. The simulation pressures, which are determined based on the tail correction of the nonbonded interactions,[71] are also given in this table. Good agreement between the experiment and force field results is obtained.

The modification to the nonbonded van der Waals parameters created minimal impact on valence parameters because the intramolecular nonbonded interaction applies only to atoms separated by at least three covalence bonds, and the "initial guess" parameters are fairly close to the "final". The most significant influence was on the torsional terms, which were slightly adjusted to yield good comparison of the conformational energies with *ab initio* results. The resulting force field, called PCFF (polymer consistent force field) in this paper, is given in the Appendix.

IV. Validation of the Force Field

The molecular structure and vibrational frequencies of disilane in the gas phase have been resolved.[57] In Table 11, the calculated normal-mode frequencies are compared with the experimental results. One can see that the scaling of the QMFF effectively corrects the systematic error in the HF/6-31G* calculations. As listed in the table, the PCFF yields very good agreements with the experiments, while the QMFF and HF/6-31G* frequencies are systematically higher than the experimental values. The molecular geometries and the rotational energy barrier of disilane are given in Table 12. The agreement between the experimental data and the PCFF results is excellent.

Conformational structures of internal rotations about three bonds, Si−Si, Si−C, and Si−C(ar), were studied. In Table 13, the conformational energies calculated for the three simplest molecules that contain these bonds, Si_4H_{10}, $Si_2H_5-C_2H_5$, and $Si_2H_5-C_6H_5$, are given. Following common convention, the dihedral angle of 180° refers to *trans*, 0° is *cis*, etc. Four conformers—*trans*, *eclipse*, *gauche*, and *cis*—were calculated for both tetrasilane (TeS) and ethyldisilane (EDS). Two structures, depending on the relative position of the phenyl ring and the Si−Si−C(ph) plane, were calculated for phenyldisilane (PDS). Due to the lack of experimental data, *ab initio* results were used to validate the derived force field in this study. Due to the limitation of computer resources, only selected conformations were calculated up to the MP2/TZ2P level of theory. The *trans* and *gauche* conformers of tetrasilane and ethyldisilane and both conformations of phenyldisilane were fully optimized; *cis* and *eclipse* conformations of tetrasilane and ethyldisilane were optimized with their dihedral angles of the backbone fixed at 0° and 120°, respectively. The conformational energies and some of the internal coordinates obtained are given in Table 13.

At the HF/6-31G* level, the lowest energy conformation of Si_4H_{10} is found to be *all-trans*, while the *gauche* conformer is 0.16 kcal/mol higher in energy than the *trans*. With a larger basis set (TZ2P), the energy difference between the *trans* and the *gauche* increases to 0.33 kcal/mol. Inclusion of electron correlation decreases the energy difference between the *trans* and *gauche*. With the 6-31G* basis set, the *gauche* confor-

Table 11. Normal-Mode Frequencies of Disilane (in cm⁻¹)

HF/6-31G*		QMFF		PCFF		
ν	$\delta\nu$	ν	$\delta\nu$	ν	$\delta\nu$	ν
2375	196	2349	170	2205	26	2179
2369	190	2345	166	2204	25	2179
2369	206	2345	182	2201	38	2163
2360	205	2344	189	2201	46	2155
2360	205	2344	189	2200	45	2155
2358	204	2349	195	2200	46	2154
1042	101	1056	115	952	11	941
1042	101	1056	115	952	11	941
1026	86	1064	124	943	3	940
1026	86	1064	124	943	3	940
1033	113	974	54	883	−37	920
948	104	964	120	873	29	844
698	70	655	27	585	−43	628
698	70	655	27	585	−43	628
465	33	453	21	423	−9	432
418	39	432	53	382	3	379
418	39	432	53	382	3	379
135		186		164		
$\lvert\delta\nu\rvert$	120		113		25	
MSD	63		63		17	

Table 12. Molecular Geometries and Energies of Disilane

	expt[57,58]	PCFF
Si−Si	2.327 (±0.005)	2.326
Si−H	1.482 (±0.002)	1.481
Si−Si−H		111.2
H−Si−H	107.85 (±0.9)	107.67
δE(Si−Si)[a]	1.26	1.14

[a] In kcal/mol.

Table 13. Comparison of Conformational Energies (in kcal/mol)

conf	HF/6-31G*	HF/TZ2P	MP2/6-31G*	MP2/TZ2P	PCFF
		Si_4H_{10}			
trans	0.0	0.0	0.0	0.0	0.0
eclipse	0.63	0.81			0.86
gauche	0.16	0.33	−0.04	0.19	0.28
cis	1.52	1.65			1.48
		$Si_2H_5-C_2H_5$			
trans	0.0	0.0	0.0	0.0	0.0
eclipse	1.67				1.24
gauche	0.15	0.20	0.02	−0.04	0.22
cis	2.01	2.16			1.60
		$Si_2H_5-C_6H_5$			
perpendicular	0.0	0.0	0.0		0.0
planar	1.04	1.06	0.74		1.04

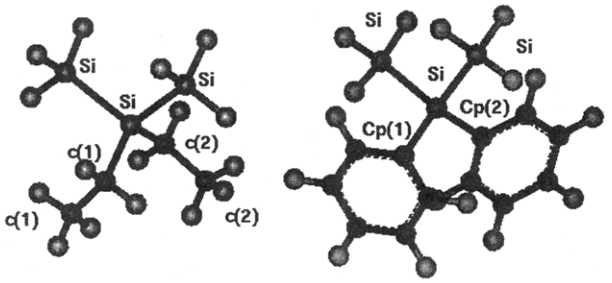

Figure 1. PCFF optimized molecular structures of diethyltrisilane and diphenyltrisilane.

mation becomes more stable than the *trans*, as indicated by a negative value in Table 13. This result agrees with that reported for similar calculations in the literature.[15] However, it is well-known that the 6-31G* basis set is not sufficient for MP2 correction.[20] In fact, at the MP2/TZ2P level, the calculated energy differences indicate that the *trans* is lower in energy by 0.19 kcal/mol than the *gauche*.

Similar results are found for the rotation about the Si−Si−C−C dihedral. At the HF/6-31G* level, the *trans* is 0.15 kcal/mol lower in energy than the *gauche*. This energy difference increases slightly when the TZ2P basis set is used. With MP2 correction, both basis sets yield very small energy differences between the *trans* and *gauche*. Comparing with the results for Si_4H_{10}, we see the *gauche* conformation is more stable in the Si−Si−C−C than in the Si−Si−Si−Si dihedral.

The energy curve of rotation about Si−C(Ph) is much simpler than the previous two cases. The perpendicular structure, in which the Si−Si bond is twisted from the phenyl ring by 90°, is the stable conformation, while the coplanar structure is a transition state of the internal rotation.

Side-chain rotation is important in order to understand the chain dynamics and conformations. Two energy maps were calculated using the present force field for diethyltrisilane and diphenyltrisilane, respectively. These maps were calculated by simultaneously rotating two Si−C bonds, while all the other degrees of freedom were relaxed. The optimized structures of these two molecules are given in Figure 1. The resulting energy maps of these two molecules are given in Figures 2 and 3, respectively. For diethyltrisilane, the two dihedral angles (ϕ_1, ϕ_2) are measured by $C^{(1)}$−Si−$C^{(2)}$−$C^{(2)}$ and $C^{(1)}$−$C^{(1)}$−Si−$C^{(2)}$. Figure 2 indicates that the global minimum-energy structure of diethyltrisilane is *gauche*−*gauche* (56°, 56°) with respect to the two dihedral angles, as shown in Figure 1; slightly higher energies are found for *trans*−*gauche* (60°, 180°) and *trans*−*trans* (180°, 180°) conformations. Overall, the *cis*−*cis* (0°, 0°) is the highest in energy. Figure 3 shows

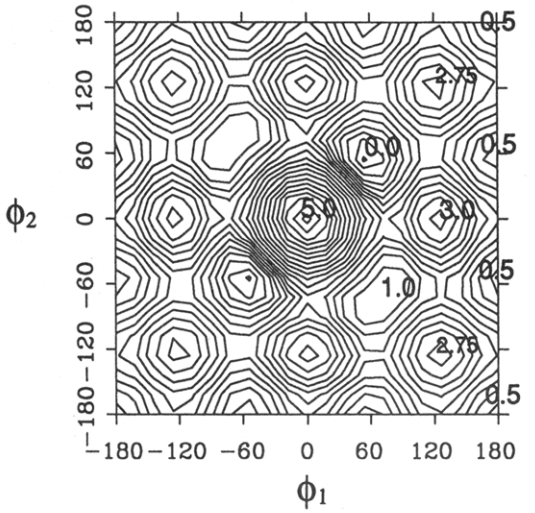

Figure 2. Minimum-energy contour of rotations about two Si−C bonds in diethylsilane, with an interval of 0.25 kcal/mol. The dihedral angles are defined by C−C−Si−C and C−Si−C−C.

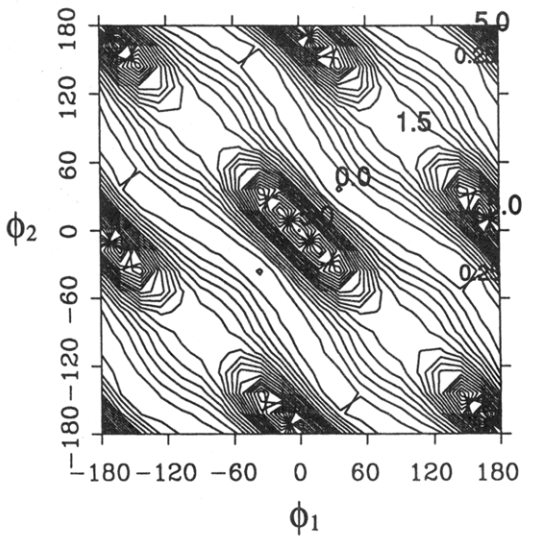

Figure 3. Minimum-energy contour of rotations about two Si−C bonds in diphenylsilane, with an interval of 0.25 kcal/mol. The dihedral angles are defined by Cp−Cp−Si−Cp and Cp−Si−Cp−Cp.

that the minimum-energy structure for diphenyltrisilane (Figure 1) is around (36°, 36°), where the dihedrals (ϕ_1, ϕ_2) are denoted by $Cp^{(1)}$−Si−$Cp^{(2)}$−$Cp^{(2)}$ and $Cp^{(1)}$−$Cp^{(1)}$−Si−$Cp^{(2)}$ (Cp refers to phenyl carbon). This is similar to that found in diphenylisopropane (a fragment of polycarbonate).[24] However, the barrier to rotation of the phenyl rings is lower in the silanes than in the carbonates; presumably because the longer Si−C bond

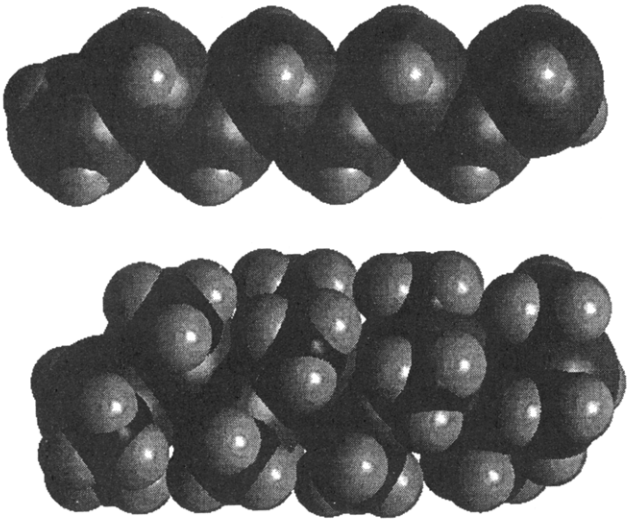

Figure 4. CPK illustration of optimized PDMS and PS. The light and small balls are hydrogens, the dark gray and large balls are silicons, and the very dark balls are carbons. The PDMS shows a helix structure in which the methyl–methyl distances are larger than those in an *all-trans* structure (not shown in the figure). The optimized PS exhibits an *all-trans* structure because the hydrogen–hydrogen distances are so large that the repulsion between the hydrogens is negligible.

Table 14. PCFF Energy Difference between the Helix and *all-trans*-PDMS (in kcal/mol)

category	$E(trans) - E$(helical)
total	2.24
nonbond	1.95
elect.	0.83
bonded	−0.57

reduces the steric force. As shown in the Figure 3, a very modest energy barrier of 0.25 kcal/mol links the two isomers.

Next, the structures of isolated polysilane (PS) and poly(dimethylsilane) (PDMS) were calculated. Since only the local structures are of interest, the calculations were performed on rather short chains: $(SiH_2)_8$ and $(Si(CH_3)_2)_8$. The optimized structures of these two molecules are given in Figure 4. As illustrated in this figure, PS has an *all-trans* backbone. This is actually a consequence of the *ab initio* results. However, the optimized PDMS shows a twisted backbone structure, with an Si–Si–Si–Si dihedral angle of 164°. This result agrees with that reported by Patnaik and Farmer,[16] who calculated the conformations using an empirical force field.

In order to understand the formation of a helical structure for isolated PDMS, a torsion-forced minimization was conducted for PDMS in which the backbone dihedral angles were fixed at 180°. By comparing the energy differences between the constrained and the optimized structures, as given in Table 14, one sees that most of the difference (1.95 of 2.24 kcal/mol) is due to the nonbonded (van der Waals) interactions.

In Figure 4, the CPK plots of the optimized structures of isolated PS and PDMS are given. The default van der Waals radii are used to define the "size" of each atom. A close examination of the optimized structure of the *trans* and the helical conformations of PDMS (Figure 5) shows that the distances between the carbons of the nearest methyl groups (those on the same side of the chain) are 3.95 and 3.97 Å in the *trans* and the helical chains, respectively, which are just on the border of the van der Waals contact distance of methane.[73] However, the shortest distances between the hydrogen atoms on the methyl groups are significantly different—2.21 Å in the *trans* and 2.54 Å in the helical chain.

As illustrated in Figure 5, the short distance between nearby hydrogen atoms in the *trans* conformation is due to the symmetry of the arrangement of methyl groups. By forming a helical conformation, the methyl groups are rotated slightly so that the distance between the hydrogens is increased. Since the short distance of 2.21 Å is smaller than the normal van der Waals diameter of the hydrogen atom,[73] the repulsion between the nearest hydrogens in the *all-trans* should be a major contribution to the energy increase.

This qualitative analysis was further tested by performing high-quality *ab initio* calculations on model methane dimers. The molecular structures and relative

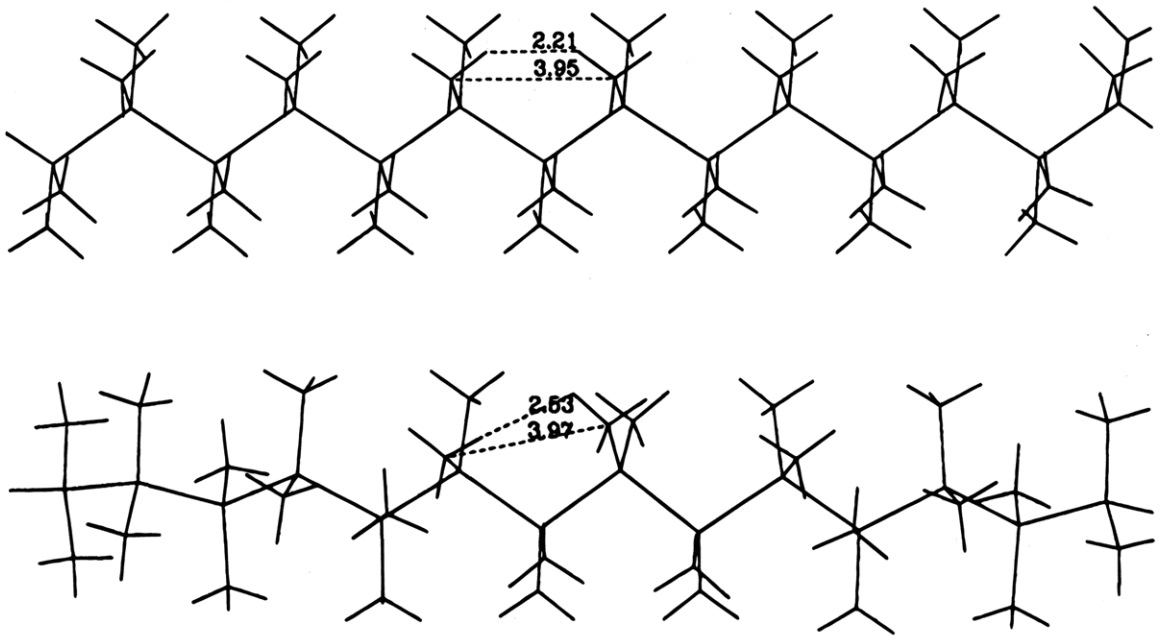

Figure 5. Illustration of optimized *trans* and helical chain conformations of PDMS. The shortest distances between hydrogen atoms are 2.21 Å in the *trans* and 2.53 Å in the helical, while the shortest distances between carbon atoms are very similar in both conformations.

Table 15. Calculated Dimerization Energies of CH_4...CH_4 Extracted from the Optimized *trans*-PDMS and Helical PDMS

method	dimer I	dimer II	$E_I - E_{II}$
HF/6-31G*	0.92	0.51	0.41
HF/TZ2P	0.96	0.52	0.44
MP2/6-31G*	0.54	0.24	0.30
MP2/TZ2P	0.21	−0.07	0.28
MP3/TZ2P	0.20	−0.07	0.27
MP4/TZ2P	0.17	−0.10	0.27
MP2/TZ2PF	0.21	−0.08	0.29
MP3/TZ2PF	0.19	−0.08	0.27
MP4/TZ2PF	0.16	−0.10	0.26

Table 16. Calculated Energy Increment from *Trans* to Helical Conformations of Tetrasilane (Si_4H_{10})

method	d*E*	method	d*E*
HF/6-31G*	0.087	HF/TZ2P	0.119
MP2/6-31G*	0.089	MP2/TZ2P	0.123

positions of the dimers were extracted from the PCFF optimized PDMS chains, with the silicon atoms replaced by hydrogens. Two conformations, denoted as I and II, are taken from the *trans* and helical chains, respectively. These structures were fixed during the calculations. The dimerization energies of these structures, calculated at different levels of theory, are given in Table 15. The dimerization energies were computed by subtracting the total energies of the dimer by the sum of the total energies of corresponding monomers at infinite separation. Hence, a positive value means the dimer, at the given conformation, is less stable than two separated monomers. The basis set superposition error (BSSE) was estimated using the counterpoise method[74-76] and subtracted from the results.

Examination of the data given in Table 15 reveals that values obtained at the HF level are all positive—the dimers in both conformations are less stable than two monomers separated at infinite distance. The dimerization energies decrease dramatically when the electron correlations are included. This is due to the fact that HF energies do not contain dispersion contributions. With triple-ζ basis sets (TZ2P, TZ2PF), MP*X* (X = 2−4) energies seem to converge to about 0.2 kcal/mol for dimer I and −0.1 kcal/mol for dimer II. In the last column of this table, the differences of the dimerization energies between the two conformations are given. Dimer I (taken from the *trans*) is less stable than dimer II (from the helical chain) by about 0.3 kcal/mol. It is of interest to point out that, although the dimerization energies calculated are highly correlated to the methods used, the energy differences between the two dimers are much less sensitive to the levels of theory.

A competing factor to the methyl−methyl repulsion between *trans* and helical chain conformation is the tendency to form an *all-trans* backbone to maximize the delocalization of the electrons—the so-called σ-conjugation effect.[1-11] In order to obtain a quantitative sense of this contribution, we calculated conformational energies of the *trans* (ϕ = 180°) and the 164°-twisted tetrasilanes. As given in Table 16, calculations up to the MP2/TZ2P level were conducted. Higher level calculations were not carried out because of the hardware limitation. However, on the basis of the calculations on disilane (see Table 1), we expect the energies obtained at the MP2/TZ2P level to be fairly close to those obtained with higher level (e.g., MP4/TZ2PF) calculations.

Examination of the data given in Table 16 shows that the *trans* is about 0.1 kcal/mol more stable than the helical conformation. Assuming this value is a good approximation of the contribution from the σ-conjugation in PDMS, we see that the methyl−methyl repulsion (which is about 0.3 kcal/mol per pair of methyl groups and four pairs are involved for each Si−Si bond rotation in PDMS) is much stronger than the force of σ-conjugation in *trans*-PDMS. The net effect of these two opposite contributions leads to the optimized helical conformation.

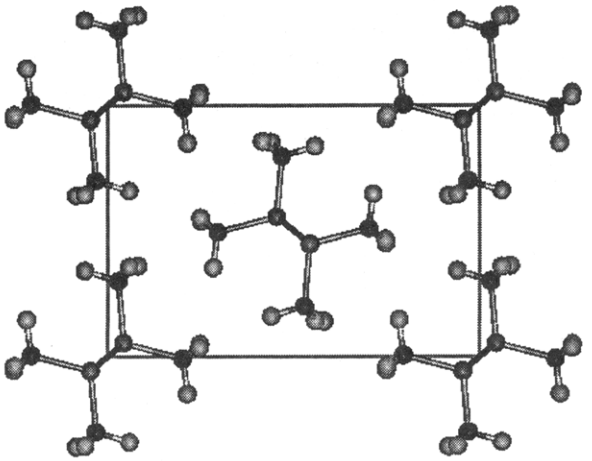

Figure 6. *ab* projection of the optimized crystal cell of PDMS. The cell parameters are given in Table 17.

Finally, crystal structures of PDMS were calculated by using the present force field. These calculations were performed on unit cells which repeat themselves in the 3D space. All degrees of freedom were relaxed during the energy minimization—not only cell parameters (a, b, c and α, β, γ) but also all internal coordinates. The nonbonded interaction is one of the major concerns in this type of calculation. Two methods were used in this study for comparison: a group-based cut-off method and a more rigorous, Ewald summation method.[77,78] In the group-based cut-off method, the nonbonded interaction is included only if the distance between the two functional groups (DMS) is shorter than a given cut-off distance. The Ewald method was performed with an accuracy of 0.001 kcal/mol.

Following the calculations reported by Patnaik and Farmer,[16] two possible packing models with *all-trans* and 15/7 helical chain conformations, respectively, were calculated. The initial packings are orthorhombic unit cells ($\alpha = \beta = \chi = 90°$) for both cases, with the chain axis parallel to the *c* direction. In the case of the *all-trans*, two chains were placed in the cell in a manner similar to the crystal structure for polyethylene (PE),[79] as illustrated in Figure 6. In the case of the 15/7 helical chain, one chain was placed at the center of the *ab* plane. Table 17 summarizes the optimized cell parameters and the total energies per repeat unit (E/RU) of these two crystalline structures.

Comparison of the cell parameters and energies calculated with different cut-off distances, and the Ewald summation shows that the results are sensitive to the approximation of nonbonded interactions. The cell parameters do not converge until the cut-off distance is 30 Å, and the energies have not converged with a cut-off of up to 50 Å, which is the maximum cut-off distance used in this study. The values calculated with cutoffs gradually approach to the values computed by Ewald summation as the cut-off distance increases. With the cut-off distance less than or equal to 20 Å, which is frequently found in many applications, significant de-

Table 17. Calculated Crystalline Cell Parameters and Energies of PDMS [CPU Time (on IBMR6000/550 Workstation) per Iteration Given in the Last Column]

method	a	b	c	α	β	γ	E/RU	CPU
				All-Trans				
cut-off								
10 Å	11.678	7.793	3.944	90.0	90.0	90.0	−0.118	0.127
20 Å	11.608	7.782	3.937	90.0	90.0	90.0	−0.654	0.521
30 Å	11.605	7.779	3.936	90.0	90.0	90.0	−0.713	1.512
40 Å	11.604	7.778	3.936	90.0	90.0	90.0	−0.724	3.952
50 Å	11.603	7.778	3.936	90.0	90.0	90.0	−0.729	7.597
Ewald	11.603	7.778	3.936	90.0	90.0	90.0	−0.735	0.386
expt[2]	12.18	8.00	3.88	90.0	90.0	91.0		
				15/7 Helix				
cut-off								
10 Å	7.499	7.423	29.045	89.6	87.4	61.3	0.350	0.338
20 Å	7.453	7.377	29.024	89.5	87.3	61.4	−0.118	1.579
30 Å	7.448	7.372	29.023	89.5	87.3	61.4	−0.175	5.813
40 Å	7.447	7.371	29.022	89.5	87.3	61.4	−0.189	13.98
50 Å	7.447	7.371	29.022	89.5	87.3	61.4	−0.193	27.12
Ewald	7.446	7.370	29.021	89.5	87.3	61.4	−0.199	1.573

viations are found for both packing models. The CPU seconds per iteration of the minimization are also given in Table 14. The computational expense of using Ewald summation (with 0.001 kcal/mol accuracy) is roughly equivalent to that of using a 20 Å cut-off distance.

The optimized *all-trans*-PDMS remains an orthorhombic packing. The calculated cell parameters are in reasonable agreement with the experimental data[2] which are also given in the same table. It is of interest to note that the cell parameters a and b are 4.7% and 2.8%, respectively, lower than the corresponding experimental values[2] that are measured at room temperature. These discrepancies are presumably due to the thermal expansions. To support this argument, one can make a comparison with the cell parameters of crystalline polyethylene (PE) measured at different temperatures—the cell parameters a and b at 4 K are about 3.9% and 1.8%, respectively, lower than the corresponding values at 303 K.[73] The optimized c parameter of *all-trans*-PDMS is slightly larger (1.4%) than the experimental value. This parameter reflects the rigidity of the molecule along the chain axis and is equivalent to the distance between the symmetry-related silicon atoms along the *all-trans* molecular axis. Comparison of the geometrical parameters optimized for the *all-trans* PDMS in both crystalline and isolated environments shows that the most significant difference is in the Si−Si bond length—it increases from 2.35 Å for the single chain to 2.37 Å for the crystal. Clearly, the nonbonded interaction has a strong impact on the Si−Si bond lengths. One can expect that a reduction of the interchain interaction (e.g., by expanding the cell along the a and b directions) may shorten the Si−Si bond length and subsequently reduce the repeat distance along the c direction.

The optimized unit cell of the helical PDMS is triclinic, $a \neq b \neq c$, $\alpha \neq \beta \neq \gamma$. Close examination of the cell parameters shows that the optimized crystal cell is similar to a hexagonal packing which was proposed by Patnaik and Farmer[16] as a stable packing model of the helical PDMS. Based on the "best" (with Ewald summation) results, the optimized helical packing is 0.531 kcal mol^{-1}/RU less stable than the *trans*, orthorhombic packing. This result qualitatively agrees with that reported by Patnaik and Farmer[16] and supports the argument that the driving force forming the *all-trans* structure of crystal PDMS is the nonbonded interaction between polymers.

V. Summary

An all-atom force field for computer simulation of polysilanes, including their alkyl and phenyl side chain derivatives, was developed based on *ab initio* calculations. The force field parameters were primarily derived by fitting to the HF/6-31G* energies, energy derivatives, and electrostatic potentials and subsequently scaled to correct the systematic calculation errors. The nonbonded van der Waals parameters were derived based on computer simulations of liquid structures and energies of simple silanes.

The reliability of using the *ab initio* methods employed in this study to predict molecular structures and conformational energies of polysilanes was investigated by performing calculations on disilane and comparing the calculated results with gas-phase experimental data. It is found that the electron correlation is crucial in predicting these properties. The best agreement between the computational and experimental results can be achieved with the MP4/TZ2PF level of theory for silanes. However, at a lower level, MP2/TZ2P calculations yield very close agreement.

Conformational structures and energies of simple silanes were studied based on *ab initio* calculations. At the MP2/TZ2P level of theory, the *trans* conformation is found to be more stable than the *gauche* alternative. The present force field yields good agreement with the high-level *ab initio* results for small, isolated silanes. On the basis of the force field assumption of transferability and additivity, the present force field was used to study the chain conformations of isolated PS and PDMS and crystalline PDMS. It has been found that the most stable chain conformation of the simple PS is *all-trans*; the isolated PDMS has a helical chain conformation due to intramolecular, nonbonded interaction between methyl groups. To directly validate the force field results of the chain conformation of PDMS from high-quality *ab initio* calculation is not feasible with our computational hardware. Alternatively, we performed the calculations on small model compounds—methane dimers and tetrasilane—to analyze the energy contributions associated with the conformational changes of PDMS. It was found that the repulsion force between two methyl groups is indeed much stronger than the stabilization force of forming an *all-trans* backbone. Finally, in the crystal packing environment, the interchain nonbonded interaction overcomes the intramolecular methyl−methyl repulsion and stabilizes the *all-trans* chain conformation.

The energy minimization of the crystalline PDMS shows the importance of using large cut-off distances or Ewald summation for the nonbonded interactions. With less than 20 Å for the cut-off distance, the neglect of long-range nonbonded interaction has a significant impact on both geometrical and energetical results. Overall, the Ewald summation method is much more efficient and accurate than the group-based cut-off method.

Provided the transferability of the force field parameters is valid, it is expected that the calculations for larger and more complex polysilanes should lead to reliable results at an accuracy similar to that presented in this paper.

Acknowledgment. This work was financially supported in part by TPL Inc., 3768 Hawkins Street NE, Albuquerque, NM 87109. The author thanks Dr. B. E. Eichinger and Dr. S. J. Mumby for reviewing the manuscript.

Appendix. Valence and Cross-Coupling Parameters (Units for the nth Force Constants are kcal/mol/Å^n for Bonds, kcal/mol/rad^n for Angles, and kcal/mol for Torsions)

Intrinsic Terms

bond	b_0 (Å)	k_2	k_3	k_4
Si–Si	2.338	114.22	−140.42	80.71
Si–H	1.478	202.78	−305.36	280.27
Si–C	1.899	189.65	−279.42	307.51
Si–Cp	1.863	233.24	−276.87	161.67

angle	θ_0 (deg)	k_2	k_3	k_4
Si–Si–H	112.09	22.51	−11.59	
H–Si–H	108.61	32.54	−8.32	
Si–Si–Si	114.27	24.95	−19.59	
H–Si–C	112.10	36.48	−12.81	
Si–C–H	112.04	28.77	−13.95	
Si–Si–C	113.00	19.47	−34.35	
C–Si–C	113.19	36.21	−20.39	20.02
Cp–Cp–Si	120.00	30.47	−23.54	
Cp–Si–H	109.59	41.95	−42.36	48.14
Si–C–C	112.67	39.52	−7.44	

torsion	k_1	k_2	k_3
–Si–Si–	0.00	0.00	−0.07
–Si–C–	0.00	0.00	−0.07
Si–Si–C–C	−0.35	0.00	−0.07
Cp–Cp–Si–*	0.00	0.00	−0.02
Si–Cp–Cp–Cp	0.00	4.33	0.00
Si–Cp–Cp–H	0.00	1.51	0.00
–C–C–	0.00	0.05	−0.14

out-of-plane[a]	k_2
Cp–Cp–Si–Cp	5.37

Cross-Coupling Terms

bond, bond	k	bond, bond	k
Si–Si/Si–Si	6.07	C–Si/Si–C	3.74
Si–Si/Si–H	3.52	Cp–Cp/Cp–Si	21.39
H–Si/Si–H	4.64	Cp–Si/Si–H	3.93
H–Si/Si–C	3.93	Si–Si/Si–C	2.30

bond, angle[b]	k	k'	bond, angle[b]	k	k'
Si–Si–H	2.07	5.66	Si–Si–C	11.44	16.95
H–Si–H	9.35	9.35	C–Si–C	18.58	18.58
Si–Si–Si	8.99	8.99	Cp–Cp–Si	14.58	23.77
H–Si–C	7.41	13.40	Cp–Si–H	22.59	8.78
Si–C–H	18.28	16.69			

angle, angle	k	angle, angle	k
H–Si–Si/Si–Si–H	1.61	Si–Si–H/H–Si–C	3.48
H–Si–H/H–Si–H	2.07	C–Si–C/C–Si–H	3.38
Si–Si–Si/Si–Si–H	4.20	C–Si–H/H–Si–C	2.80
Si–Si–H/H–Si–Si	3.49	Si–Si–Si/Si–Si–C	4.53
H–Si–H/H–Si–C	4.46	C–Si–Si/Si–Si–C	2.08
H–Si–C/C–Si–H	4.68	Si–Si–C/C–Si–Si	−5.68
H–C–Si/Si–C–H	2.21	Si–Si–C/C–Si–C	1.35
H–Si–Si/Si–Si–C	−2.96		

torsion, bond[c]	k_1	k_2	k_3
H–Si–Si–H	0.00	0.00	−0.63
H–Si–C–H	0.00	0.00	−0.59
H–Si–Si–C	0.00	0.00	−0.69
Si–Si–C–H	0.00	0.00	−0.19
Si–Cp–Cp–Cp	0.00	11.16	0.00
Si–Cp–Cp–H	0.00	6.22	0.00
Cp–Cp–Si–H	0.00	0.00	−0.31

angle, torsion[d]	k_1	k_2	k_3	k'_1	k'_2	k'_3
Si–Cp–Cp–Cp	0.00	4.33	0.00	0.00	−5.54	0.00
Si–Cp–Cp–H	0.00	1.111	0.00	0.00	4.59	0.00
Cp–Cp–Si–H	0.00	0.000	−0.28	0.000	0.00	−0.19

angle, torsion, angle	k	angle, torsion, angle	k
H–Si–Si–H	−10.82	H–Si–Si–C	−16.91
H–Si–Si–Si	−12.29	Si–Si–C–H	−13.37
H–Si–C–H	−12.93	C–Si–C–H	−17.58

[a] The out-of-plane angle is defined by i–j–k–l, where j is the center atom to which atoms i, k, and l are bonded. [b] Two bond–angle terms are given for (i,j,k); the angle is defined by i–j–k; two bonds are defined by i–j (b) and j–k (b'), respectively. [c] The torsion angle is defined by i–j–k–l; the bond is defined by j–k. [d] The torsion angle is defined by i–j–k–l; two angles are defined by i–j–k and j–k–l, respectively.

References and Notes

(1) Lovinger, A. J.; Davis, D. D.; Schilling, F. C.; Padden, F. J.; Bovey, F. A.; Zeigler, J. M. *Macromolecules* **1991**, *24*, 132.
(2) Lovinger, A. J.; Davis, D. D.; Schilling, F. C.; Bovey, F. A.; Zeigler, J. M. *Polym. Commun.* **1989**, *30*, 356.
(3) Miller, R. D.; Farmer, B. L.; Fleming, W.; Sooriyakumaran, R.; Rabolt, J. F. *J. Am. Chem. Soc.* **1987**, *109*, 2509.
(4) Schilling, F. C.; Lovinger, A. J.; Zeigler, J. M.; Davis, D. D.; Bovey, F. A. *Macromolecules* **1989**, *22*, 3055.
(5) Kuzmany, H.; Rabolt, J. F.; Farmer, B. L.; Miller, R. D. *J. Chem. Phys.* **1986**, *85*, 7413.
(6) Rabolt, J. F.; Hofer, D.; Miller, R. D.; Fickes, G. N. *Macromolecules* **1986**, *19*, 611.
(7) Harrah, L. A.; Zeigler, J. M. *J. Polym. Sci., Polym. Lett. Ed.* **1985**, *23*, 209.
(8) Harrah, L. A.; Zeigler, J. M. *Bull. Am. Phys. Soc.* **1985**, *30*, 540.
(9) Harrah, L. A.; Zeigler, J. M. *Macromolecules* **1987**, *20*, 601.
(10) Trefonas, P.; Damewood, J. R.; West, R.; Miller, R. D. *Organometallics* **1985**, *4*, 1318.
(11) Schweizer, K. S.; Harrah, L. A.; Zeigler, J. M. Silicon Based Polymer Science. *Adv. Chem. Ser.* **1990**, *224*, 379.
(12) Damewood, J. R.; West, R. *Macromolecules* **1985**, *18*, 158.
(13) Cui, C. X.; Karpfen, A.; Kertesz, M. *Macromolecules* **1990**, *23*, 3302.
(14) Welsh, W. J.; Johnson, W. D. *Macromolecules* **1990**, *23*, 1881.
(15) Mintmire, J. W.; Ortiz, J. V. *Macromolecules* **1988**, *21*, 1191. Ortiz, J. V.; Mintmire, J. W. *J. Am. Chem. Soc.* **1988**, *110*, 4522.
(16) Patnaik, S. S.; Farmer, B. L. *Polymer* **1992**, *33*, 5121.
(17) Dewar, M. J. S.; Thiel, W. *J. Am. Chem. Soc.* **1977**, *99*, 4899.
(18) Dewar, M. J. S.; Zoebisch, E. G.; Healy, E. F.; Stewart, J. J. P. *J. Am. Chem. Soc.* **1985**, *107*, 3902.
(19) Stewart, J. J. P. *J. Comput. Chem.* **1989**, *10*, 221.
(20) Hehre, W. J.; Radom, L.; Schleyer, P. v. R.; Pople, J. A. *Ab Initio Molecular Orbital Theory*; John Wiley & Sons: New York, 1986; and references therein.
(21) Allinger, N. L.; Grev, V. S.; Yates, B. F.; Schaefer, H. F.; *J. Am. Chem. Soc.* **1990**, *112*, 114.
(22) Burkert, U.; Allinger, N. L. *Molecular Mechanics*; American Chemical Society: Washington, D.C., 1982.
(23) Weiner, S. J.; Kollman, P. A.; Nguyen, D. T.; Case, D. A. *J. Comput. Chem.* **1986**, *7*, 230.
(24) Dauber-Osguthorpe, P.; Roberts, V. A.; Osguthorpe, D. J.; Wolff, J.; Genest, M.; Hagler, A. T. *Proteins: Struct., Funct., Genet.* **1988**, *4*, 31.
(25) Nilsson, L.; Karplus, M. *J. Comput. Chem.* **1990**, *7*, 591.
(26) Allinger, N. L.; Yuh, Y. H.; Lii, J. H. *J. Am. Chem. Soc.* **1989**, *23*, 8551.
(27) Maple, J. A.; Hwang, M. J.; Stockfisch, T. P.; Dinur, U.; Waldman, M.; Ewig, C. S.; Hagler, A. T. *J. Comput. Chem.* **1994**, *15*, 162.
(28) Hwang, M. J.; Stockfisch, T. P.; Hagler, A. T. *J. Am. Chem. Soc.* **1994**, *116*, 2515.
(29) Sun, H.; Mumby, S. J.; Maple, J. R.; Hagler, A. T. *J. Am. Chem. Soc.* **1994**, *116*, 2978.
(30) Sun, H. *J. Comput. Chem.* **1994**, *15*, 752.
(31) Lii, J. H.; Allinger, N. L. *J. Am. Chem. Soc.* **1989**, *111*, 8566.
(32) Allinger, N. L.; Li, F. B.; Yan, L. Q.; Tai, J. C. *J. Comput. Chem.* **1990**, *11*, 868.
(33) Allinger, N. L.; Li, F. B.; Yan, L. Q. *J. Comput. Chem.* **1990**, *11*, 848.
(34) Lii, J. H.; Allinger, N. L. *J. Comput. Chem.* **1991**, *12*, 186.
(35) Allinger, N. L.; Kuang, J. X.; Thomas, H. D. *J. Mol. Struct.: THEOCHEM* **1990**, *68*, 125.
(36) Allinger, N. L.; Rahman, M.; Lii, J. H. *J. Am. Chem. Soc.* **1990**, *112*, 8293.
(37) Schmitz, L. R.; Allinger, N. L. *J. Am. Chem. Soc.* **1990**, *112*, 8307.
(38) Allinger, N. L.; Chen, K. S.; Rahman, M.; Pathiaseril, A. *J. Am. Chem. Soc.* **1991**, *113*, 4505.
(39) Allinger, N. L.; Quinn, M.; Rahman, M.; Chen, K. H. *J. Phys. Org. Chem.* **1991**, *11*, 647.
(40) Chen, K. H.; Allinger, N. L. *J. Phys. Org. Chem.* **1991**, *11*, 659.
(41) Gough, C. A.; Debolt, S. E.; Kollman, P. A. *J. Comput. Chem.* **1992**, *13*, 963.
(42) Smith, J. C.; Karplus, M. *J. Am. Chem. Soc.* **1992**, *114*, 801.
(43) Rappé, A. K.; Casewit, C. J.; Colwell, K. S.; Goddard, W. A.; Skiff, W. M. *J. Am. Chem. Soc.* **1992**, *114*, 10024.
(44) Rappé, A. K.; Goddard, W. A. *J. Phys. Chem.* **1991**, *95*, 3358.
(45) Wendel, J. A.; Goddard, W. A. *J. Chem. Phys.* **1992**, *97*, 5048.
(46) Karasawa, N.; Dasgupta, S.; Goddard, W. A. *J. Phys. Chem.* **1991**, *21*, 2260.

(47) Karasawa, N.; Goddard, W. A. *Macromolecules* **1992**, *25*, 7268.
(48) Mayo, S. L.; Olafson, B. D.; Goddard, W. A. *J. Phys. Chem.* **1990**, *94*, 8897.
(49) Amodeo, P.; Barone, V. *J. Am. Chem. Soc.* **1992**, *114*, 9085.
(50) Haeser, M.; Ahlrichs, R. *J. Comput. Chem.* **1989**, *10*, 104. Ahlrichs, R.; Baer, M.; Haeser, M.; Horn, H.; Koelmel, C. *Chem. Phys. Lett.* **1989**, *162*, 165. This program is distributed by Biosym Technologies, Inc.
(51) GAUSSIAN90 is distributed by Gaussian Inc., Pittsburgh, PA, 1991.
(52) DISCOVER and PROBE are distributed by Biosym Technologies, Inc., San Diego, CA, 1994.
(53) Hehre, W. J.; Ditchfield, R.; Pople, J. A. *J. Chem. Phys.* **1972**, *56*, 2257. Hariharam, P. C.; Pople, J. A. *Theor. Chim. Acta* **1973**, *28*, 213.
(54) Schäfer, A.; Horn, H.; Ahlrichs, R. *J. Chem. Phys.* **1992**, *97*, 2571.
(55) Pople, J. A.; Seeger, R.; Krishnan, R. *Int. J. Quantum Chem.* **1977**, *11S*, 149. Krishnan, R.; Pople, J. A. *Int. J. Quantum Chem.* **1978**, *14*, 91.
(56) Turbomole User Guide, V2.3, Biosym Technologies, 1994.
(57) Durig, J. R.; Church, J. S. *J. Chem. Phys.* **1980**, *73*, 4784. Shotton, K. C.; Lee, A. G.; Jones, W. J. *J. Raman Spectrosc.* **1973**, 243.
(58) *Gmelin Handbook of Inorganic Chemistry*, 8th ed.; Springer-Verlag: New York, 1982; No. 15.
(59) Hagler, A. T.; Lifson, S.; Dauber, P. *J. Am. Chem. Soc.* **1979**, *101*, 5122.
(60) Williams, D. E.; Yan, J.-M. *Advances in Atomic and Molecular Physics*; Academic Press: New York, 1988; Vol. 23, p 87.
(61) Williams, D. E. *J. Comput. Chem.* **1988**, *9*, 745.
(62) Williams, D. E. *Biopolymers* **1990**, *29*, 1367.
(63) Colonna, F.; Ángyán, J. G.; Tapia, O. *Chem. Phys. Lett.* **1990**, *172*, 55.
(64) Breneman, C. M.; Wiberg, K. B. *J. Comput. Chem.* **1990**, *3*, 361.
(65) Colonna, F.; Evleth, E.; Ángyán, J. G. *J. Comput. Chem.* **1992**, *13*, 1234.
(66) Urban, H. J.; Famini, G. R. *J. Comput. Chem.* **1993**, *14*, 353.
(67) Hirschfeld, F. L. *Theor. Chim. Acta* **1977**, *44*, 129.
(68) Coppens, P.; Stevens, E. D. *Adv. Quantum Chem.* **1977**, *10*, 1.
(69) Besler, B. H.; Merz, K. M.; Kollman, P. A. *J. Comput. Chem.* **1990**, *11*, 431.
(70) Sun, H. Unpublished results.
(71) Rigby, D. Private communication.
(72) Davidson, E. R.; Feller, D. *Chem. Rev.* **1986**, *86*, 681.
(73) Hirschfelder, J. O.; Curtiss, C. F.; Bird, R. B. *Molecular Theory of Gases and Liquids*; Wiley: New York, 1954.
(74) Boy, S. F.; Bernardi, F. *Mol. Phys.* **1970**, *553*, 19.
(75) Michael, D. W.; Dykstra, C. E.; Lisy, J. M. *J. Chem. Phys.* **1984**, *81*, 2535.
(76) Trular, D. G.; Schwenke, W. *J. Chem. Phys.* **1985**, *82*, 2418.
(77) Tosi, M. P. *Solid State Phys.* **1964**, *16*, 107.
(78) *Discover 2.9.5/94.0 User Guide*, Biosym Technologies, Inc., 1994.
(79) Tadokoro, H. *Structure of Crystalline Polymers*; Robert E. Krieger Publishing Co.: Malabar, FL, 1990.

MA9411181